

Shear wave propagation in magneto poroelastic medium sandwiched between self-reinforced poroelastic medium and poroelastic half space

Sindhuja Ala, Rajitha Gurijala and Malla Reddy Perati
Department of Mathematics, Kakatiya University, Warangal, India

Received 5 November 2019
Revised 6 April 2020
16 April 2020
Accepted 21 April 2020

Abstract

Purpose – The purpose of this paper is to investigate the effect of reinforcement, inhomogeneity and initial stress on the propagation of shear waves. The problem consists of magneto poroelastic medium sandwiched between self-reinforced medium and poroelastic half space. Using Biot's theory of wave propagation, the frequency equation is obtained.

Design/methodology/approach – Shear wave propagation in magneto poroelastic medium embedded between a self-reinforced medium and poroelastic half space is investigated. This particular setup is quite possible in the Earth crust. All the three media are assumed to be inhomogeneous under initial stress. The significant effects of initial stress and inhomogeneity parameters of individual media have been studied.

Findings – Phase velocity is computed against wavenumber for various values of self-reinforcement, heterogeneity parameter and initial stress. Classical elasticity results are deduced as a particular case of the present study. Also in the absence of inhomogeneity and initial stress, frequency equation is discussed. Graphical representation is made to exhibit the results.

Originality/value – Shear wave propagation in magneto poroelastic medium embedded between a self-reinforced medium, and poroelastic half space are investigated in presence of initial stress, and inhomogeneity parameter. For heterogeneous poroelastic half space, the Whittaker's solution is obtained. From the numerical results, it is observed that heterogeneity parameter, inhomogeneity parameter and reinforcement parameter have significant influences on the wave characteristics. In addition, frequency equation is discussed in absence of inhomogeneity and initial stress. For the validation purpose, numerical results are also computed for a particular case.

Keywords Shear wave, Self-reinforcement, Magneto poroelastic, Half-space, Inhomogeneity, Initial stress

Paper type Research paper

1. Introduction

Study of mechanical behavior of self-reinforced material has a huge importance in the domains such as structural engineering and geomechanics. Self-reinforced materials attract many

Authors acknowledge Department of Science and Technology (DST) for funding through Fund for Improvement of S&T Infrastructure (FIST) program sanctioned to the Department of Mathematics, Kakatiya University, Warangal with File No. SR/FST/MSI-101/2014. One of the authors Rajitha Gurijala acknowledges University Grants Commission (UGC), Government of India, for its financial support through the Postdoctoral Fellowship for Women (Grant Number F.15–1/2015–17/PDFWM-2015–17-TEL-34525 (SA-II)).



investigators in the field of engineering applications due to their superiority over other structural materials in the applications where high strength and stiffness and light weight components are required. Most of the structures on or near the surface of the Earth are self-reinforced and are constructed in such a manner that the effect of earthquake or similar disturbances causes minimum destruction. Many elastic fiber-reinforced composite materials are strongly anisotropic in nature. There are many materials for example, the Earth's crust and mantle which are inhomogeneous. The Earth crust contains some hard and soft rocks that exhibit both self-reinforcement property and inhomogeneity. As a result of stress developed within the crust, deformation takes place along with fracture. These fractures release large amount of energy which give rise to elastic waves travel and finally reach to surface. Moreover, the Earth crust made of diversity of igneous, metamorphic and sedimentary rocks. These rocks are capable to generate magnetic field due to presence of some minerals like iron, nickel and cobalt in them. For the said reasons, these rocks can be treated as magneto poroelastic solids. An increasing attention is being devoted to the interactions between magnetic and strain fields. Belfield *et al.* (1983) introduced the continuous reinforcement at every point of an elastic solid. Vardoulakis (1984) studied the propagation of torsional surface waves in heterogeneous elastic media. Propagation of shear waves and transverse surface waves in self-reinforced magneto elastic bodies is investigated by Verma (1986) and Verma *et al.* (1988). Chattopadhyay and Chaudhary (1995) discussed the propagation of magneto elastic shear waves in an infinite self-reinforced plate. Chaudhary *et al.* (2006) reveal that reflection and transmission coefficients are strongly influenced by the reinforcement parameters, and angle of incidence of the incident wave. Chattopadhyay *et al.* (2010) investigated the dispersion of shear wave in multilayered magneto elastic self-reinforced media. Effects of point source, self-reinforcement and heterogeneity on the propagation of magneto elastic shear waves are presented in Chattopadhyay *et al.* (2011). Samal and Chattaraj (2011) discussed the surface wave propagation in fiber-reinforced anisotropic elastic layer between liquid saturated porous half space and uniform liquid layer. Propagation of shear waves in an irregular self-reinforcement layer, the combined effects of reinforcement, magnetic field and irregularity are studied by Chattopadhyay and Kumar (Chattopadhyay and Singh, 2012). Chattopadhyay *et al.* (2012) discussed the torsional surface waves in a self-reinforced medium over a heterogeneous half space. Using the dual reciprocity boundary element method (DRBEM), Fahmy (2012a, 2012b, 2012c, 2012d) studied the transient magneto-thermo-viscoelastic stresses in a non-homogeneous anisotropic solid subjected to a heat source. The effect of a moving heat source on the transient magneto-thermo-visco-elastic stresses in a non-homogeneous anisotropic solid is investigated (Fahmy, 2012a, 2012b, 2012c, 2012d). Fahmy (2012a, 2012b, 2012c, 2012d) discussed the generalized magneto thermoelasticity problem of rotating anisotropic viscoelastic functionally graded solids. Generalized magneto-thermo viscoelastic problem of rotating functionally graded materials are investigated by Fahmy (2012a, 2012b, 2012c, 2012d) and Fahmy (2013). Abd-Alla *et al.* studied the surface waves propagation in fiber-reinforced anisotropic elastic media subjected to gravitational field (Abd-Alla *et al.*, 2013). Chattaraj and Samal studied the propagation of Love waves in fiber-reinforced layer lying over a gravitating anisotropic porous half space (Chattaraj and Samal, 2013). From Chattaraj and Samal (2013), authors concluded that the transverse and longitudinal rigidity of reinforced material, and porosity of half space have a significant effect on wave propagation. Chatterjee *et al.* (2015) studied the propagation of shear waves in visco-elastic heterogeneous layer overlying on initially stressed half space. Effect of reinforcement on half-space is discussed (Singh *et al.*, 2016). Tong *et al.* (2016) investigated wave propagation characteristics in fluid saturated porous materials in the framework of nonlocal Biot's theory. By considering the interface between self-reinforced medium and half space, effect of reinforcement and heterogeneity on the propagation

of torsional surface waves is discussed by [Paswan *et al.* \(2017\)](#). Effect of gravity and initial stress on propagation of torsional surface waves in heterogeneous medium is studied ([Mukhopadhyay *et al.*, 2017](#)). The reflection of plane waves in a rotating magneto elastic fibre-reinforced semi space is investigated by [Roy *et al.* \(2017\)](#). From [Roy *et al.* \(2017\)](#), it is clear that magnetic field, rotation, fibre-reinforcement and surface stress play vital role in wave propagation, particularly, in reflection of plane waves. Using Biot's theory ([Biot, 1956](#)), shear wave propagation in magneto poroelastic dissipative isotropic medium sandwiched between two poroelastic half spaces is studied ([Balu *et al.*, 2017](#)). In [Balu *et al.* \(2017\)](#), wave characteristics are computed at the fixed heterogeneous and magnetic poroelastic coupling factor. [Tong *et al.* \(2018\)](#) studied the Rayleigh wave propagation in porous fluid saturated materials and concluded that the nonlocal parameter does not have significant influence on the characteristics of Rayleigh waves within a low frequency range when compared to that of classical Biot theory. Effect of several parameters of reinforced sandwich porous plates such as aspect ratios, volume fraction, types of reinforcement and thickness of plate on bending is investigated by [Medani *et al.* \(2019\)](#). The nonlinear static, buckling and vibration analysis of viscoelastic micro-composite beam reinforced by various distributions of boron nitride nanotube (BNNT) is studied by using finite element method (FEM) ([Alimirzaei *et al.*, 2019](#)). Vibration analysis of functionally graded micro beams is studied by [Tlidji *et al.* \(2019\)](#). [Boukhelif *et al.* \(2019\)](#) made dynamic investigation of functionally graded (FG) plates resting on an elastic foundation using a simple quasi-3D HSPT in which the stretching effect is considered. Some recent papers ([Karami *et al.*, 2019a, 2019b](#); [Karami *et al.*, 2019a, 2019b](#)) are reported in the field of the functionally graded nanoplates reinforced with graphene nanoplates and nanoshell in magnetic field. In the above-mentioned papers, the authors have not studied the wave propagation in magneto poroelastic medium sandwiched between self-reinforced medium and poroelastic half space. Hence, in the present work, the same is investigated. This particular setup is quite possible in the Earth's crust. All the three media are assumed to be inhomogeneous under initial stress. The significant effects of initial stress, and inhomogeneity parameters of the individual media have been studied.

This paper is organized as follows. In Section 2, formulation of the problem is given. The solution of the problem is discussed in Section 3. Boundary conditions and frequency equation are presented in Section 4. In Section 5, particular cases are discussed. Numerical results are described in Section 6. Finally, conclusion is given in Section 7.

2. Formulation of the problem

Consider the magneto poroelastic medium sandwiched between inhomogeneous self-reinforced medium and poroelastic half space, all assumed to be under initial stress. The origin O is considered in a manner such that it separates the sandwiched layer from upper and lower half-spaces. The horizontal axis is assumed to be along r -axis, and z -axis is in downward direction as shown in [Figure 1](#). From the figure, it is clear that upper self-reinforcement layer M_1 (say), magneto poroelastic layer M_2 (say), and poroelastic half space M_3 (say) occupy the spaces $(-h_2 < z < -h_1)$, $(-h_1 < z < 0)$ and $(z > 0)$, respectively. Equations of motion for shear deformation in the isotropic poroelastic medium in absence of dissipation are ([Biot, 1956](#))

$$\begin{aligned} N \left(\nabla^2 - \frac{1}{r^2} + \frac{2}{r^2} \frac{\partial}{\partial \theta} \right) v + (A + N) \frac{\partial e}{\partial r} + Q \frac{\partial \varepsilon}{\partial r} &= \frac{\partial^2}{\partial t^2} (\rho_{11} v + \rho_{12} V), \\ \frac{Q}{r} \frac{\partial e}{\partial \theta} + \frac{R}{r} \frac{\partial \varepsilon}{\partial \theta} &= \frac{\partial^2}{\partial t^2} (\rho_{12} v + \rho_{22} V). \end{aligned} \quad (1)$$

In [equation \(1\)](#), v and V are the displacement components of solid and fluid, respectively, $P = A + 2N, Q$, and R are all poroelastic constants, e and ε are the dilatations of solid and

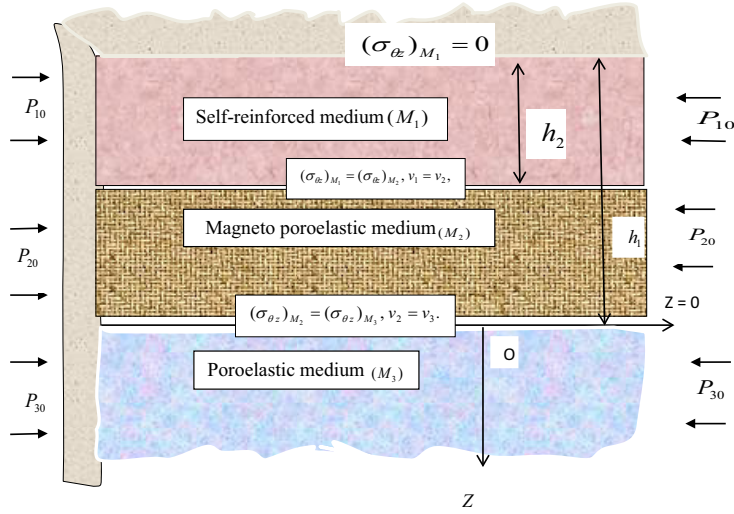


Figure 1.
Geometry of the
problem

fluid. The mass coefficients ρ_{11}, ρ_{12} and ρ_{22} satisfy the relations $\rho_1 = \rho_{11} + \rho_{12} = (1-\beta)\rho_s$, $\rho_2 = \rho_{12} + \rho_{22} = \beta\rho_f$, $\rho = \rho_1 + \rho_2 = \rho_s + \beta(\rho_f - \rho_s)$. Here, ρ_1 and ρ_2 are masses of solid and fluid per unit volume of aggregate, ρ is total mass of solid-fluid aggregate per unit volume. ρ_s and ρ_f are mass densities of the solid and fluid, respectively. β is the porosity of the aggregate. The solid stresses σ_{ij} , and fluid pressure s are given by (Biot, 1956):

$$\sigma_{ij} = 2Ne_{ij} + (Ae + Q\varepsilon)\delta_{ij}, \quad (i, j = 1, 2, 3), \quad s = Qe + R\varepsilon. \quad (2)$$

In equation (2), e'_{ij} s are strain components, and δ_{ij} is the well-known Kronecker delta function.

3. Solution of the problem

The solutions for three medium are presented in the following sub sections.

3.1 Upper self-reinforced medium ($-h_2 < z < -h_1$)

Let (u_1, v_1, w_1) and (U_1, V_1, W_1) be the displacement components of solid and fluid, respectively, in the upper self-reinforced medium. For the shear vibrations, displacement components are $u_1 = w_1 = 0$, $v_1 = v_1(r, z, t)$, and $U_1 = W_1 = 0$, $V_1 = V_1(r, z, t)$. The stress tensor for a self-reinforced medium along the preferred direction \vec{a} is given below (Chattopadhyay et al., 2011).

$$\begin{aligned} \sigma_{ij} = & \lambda e_{kk}\delta_{ij} + 2\mu_T e_{ij} + \alpha(a_k a_l e_{kl}\delta_{ij} + a_i a_j e_{kk}) + 2(\mu_L - \mu_T)(a_i a_k e_{kj} + a_j a_k e_{ki}) \\ & + \beta a_k a_m e_{km} a_i a_j, \end{aligned}$$

Here, $i, j, k, l, m = 1, 2, 3$, and the coefficients $\lambda, \alpha, \beta, \mu_T, \mu_L$ are the elastic constants with the dimension of stress, μ_T and μ_L are the transverse and longitudinal shear modulus, respectively, the vector $\vec{a} = (a_1, a_2, a_3)^T$ is the preferred unit direction of reinforcement so

that $a_1^2 + a_2^2 + a_3^2 = 1$. In the plane under consideration, $\vec{a}_i = (\sin \phi, 0, \cos \phi)^T$, ϕ is the angle of inclination to the radial axis. For torsional vibrations, the strain components are as follows:

$$e_{rr} = e_{\theta\theta} = e_{zz} = e_{zr} = 0, e_{\theta z} = \frac{1}{2} \frac{\partial v}{\partial z}, \text{ and } e_{r\theta} = \frac{1}{2} \left(\frac{\partial v}{\partial r} - \frac{v}{r} \right).$$

Using the above in [equation \(2\)](#), the non-zero stress components are given by:

$$\sigma_{r\theta} = \mu_T \left[S_1 \left(\frac{\partial v}{\partial r} - \frac{v}{r} \right) + S_2 \frac{\partial v}{\partial z} \right], \sigma_{\theta z} = \mu_T \left[S_2 \left(\frac{\partial v}{\partial r} - \frac{v}{r} \right) + S_3 \frac{\partial v}{\partial z} \right]. \quad (3)$$

In [equation \(3\)](#), $S_1 = \left(1 + (\mu' - 1)a_1^2 \right)$, $S_2 = (\mu' - 1) a_1 a_3$, $S_3 = 1 + (\mu' - 1)a_3^2$, $\mu' = \frac{\mu_L}{\mu_T}$, $\mu_L = \mu_{L_0} e^{az}$, $\mu_T = \mu_{T_0} e^{az}$.

In this case, the equations of motion are:

$$\begin{aligned} \frac{\partial}{\partial r}(\sigma_{r\theta}) + \frac{\partial}{\partial z}(\sigma_{\theta z}) + \frac{2}{r}(\sigma_{r\theta}) - \frac{\partial}{\partial z}(P_1 e_{\theta z}) &= \frac{\partial^2}{\partial t^2}(\rho_{11} v_1 + \rho_{12} V_1), \\ 0 &= \frac{\partial^2}{\partial t^2}(\rho_{12} v_1 + \rho_{22} V_1). \end{aligned} \quad (4)$$

Because of the inhomogeneity with respect to the z coordinate the following are assumed in [equation \(4\)](#), P_1 denotes the initial stress, and $P_1 = P_{10} e^{az}$, $\rho_{11} = \rho_{110} e^{az}$, $\rho_{12} = \rho_{120} e^{az}$, $\rho_{22} = \rho_{220} e^{az}$, here a is a constant, $P_{10}, \rho_{110}, \rho_{120}, \rho_{220}$, are the values of their respective parameters at $z = 0$. For harmonic waves, the displacement component $v_1(z)$ is assumed as:

$$v_1(z) = f_1(z) J_1(kr) e^{i\omega t}, \quad (5)$$

Here, $k, c, \omega (=kc)$ and $J_1(\cdot)$ are wavenumber, wave velocity, circular frequency and Bessel's function of first order and first kind, respectively. From [equations \(3\), \(4\) and \(5\)](#), the following equation is obtained:

$$\frac{d^2 f_1}{dz^2} + E \frac{df_1}{dz} + F f_1 = 0. \quad (6)$$

In [equation \(6\)](#),

$$E = \frac{M_{20} k J_1'(kr)}{M_{40} J_1(kr)} + \frac{M_{60}}{M_{40}},$$

$$\begin{aligned} F &= \frac{M_{10} J_1'(kr) k^2}{M_{40} J_1(kr)} + \frac{M_{10} J_1(kr) k}{r M_{40} J_1(kr)} + \frac{a M_{20} J_1'(kr) k}{M_{40} J_1(kr)} - \frac{M_{10}}{r^2 M_{40}} - \frac{a M_{20}}{r M_{40}} \\ &\quad + \omega^2 \left(\frac{\rho_{110} \rho_{220} - \rho_{120}^2}{\rho_{220} \mu_{T_0} M_{40} J_1(kr)} \right), \end{aligned}$$

$$\begin{aligned} M_{10} &= 1 + (\mu'_0 - 1) a_1^2, \quad M_{20} = (\mu'_0 - 1) a_1 a_3, \quad M_{60} = (M_{20}/r) + a M_{40}, \quad M_{40} = (M_{30} - \xi_{10}), \\ M_{30} &= 1 + (\mu'_0 - 1) a_3^2, \quad \xi_{10} = P_{10}/2\mu_{T_0}. \end{aligned}$$

Substitution of the solution of [equation \(6\)](#) in [equation \(5\)](#) gives:

$$v_1(z) = \exp(-Ez/2) (C_1 \cos(\chi_1 z) + C_2 \sin(\chi_1 z)) J_1(kr) e^{i\omega t}. \quad (7)$$

In [equation \(7\)](#), $\chi_1^2 = F - \frac{E^2}{4}$, C_1, C_2 are arbitrary constants. The pertinent stress component $\sigma_{\theta z}$ is given by:

$$\begin{aligned} (\sigma_{\theta z})_{M_1} = & C_1 \left(\mu_T S_2 k \sin(\chi_1 z) J_1'(kr) - S_2 \mu_T \sin(\chi_1 z) \frac{J_1(kr)}{r} + S_3 \cos(\chi_1 z) \chi_1 J_1(kr) \right. \\ & \left. - S_3 \frac{E}{2} \sin(\chi_1 z) J_1(kr) \right) + C_2 \left(\mu_T S_2 k \cos(\chi_1 z) J_1'(kr) - \mu_T S_2 \cos(\chi_1 z) \frac{J_1(kr)}{r} \right. \\ & \left. + S_3 \sin(\chi_1 z) \chi_1 J_1(kr) - S_3 \frac{E}{2} \cos(\chi_1 z) J_1(kr) \right). \end{aligned}$$

3.2 The sandwiched magneto poroelastic medium ($-h_1 < z < 0$)

Let (u_2, v_2, w_2) and (U_2, V_2, W_2) be the solid and fluid displacement components, respectively, in the sandwiched magneto poroelastic medium. For shear wave, [equation \(1\)](#) takes the following form:

$$\begin{aligned} \frac{\partial \sigma_{r\theta}}{\partial r} + \frac{1}{r} \frac{\partial \sigma_{\theta\theta}}{\partial \theta} + \frac{\partial \sigma_{\theta z}}{\partial z} + \frac{2\sigma_{r\theta}}{r} + P_2 \frac{\partial w_r}{\partial z} + (\vec{J} \times \vec{B})_\theta &= \frac{\partial^2}{\partial t^2} (\rho_{1100} v_2 + \rho_{1200} V_2), \\ 0 &= \frac{\partial^2}{\partial t^2} (\rho_{1200} v_2 + \rho_{2200} V_2). \end{aligned} \quad (8)$$

In [equation \(8\)](#), $(\vec{J} \times \vec{B})_\theta$ is the θ component of electromagnetic force, \vec{J} is the electric current density and \vec{B} is the magnetic induction vector. The Maxwell's equations of the electromagnetic field are ([Balu et al., 2017](#)):

$$\vec{\nabla} \cdot \vec{B} = 0, \vec{\nabla} \times \vec{E} = -\frac{\partial \vec{B}}{\partial t}, \vec{\nabla} \times \vec{H} = \vec{J}, \vec{B} = \mu_e \vec{H}, \vec{J} = \sigma \left(\vec{E} + \frac{\partial v}{\partial t} \times \vec{B} \right), \quad (9)$$

here, \vec{E} is the induced electric field, \vec{H} is the magnetic field consisting both primary and induced magnetic field, μ_e and σ are the induced permeability and conduction coefficient, respectively. The Maxwell stress tensor $(\tau_{ij}^0)^{M_x} = \mu_e (H_i p_j - H_j p_i - H_k p_k \delta_{ij})$. Let $\vec{H} = (H_r, H_\theta, H_z)$ and change in magnetic field be (P_1, P_2, P_3) . If the displacement current is absent, then [equation \(9\)](#) reduces to:

$$\nabla^2 H = \mu_e \sigma \left(\frac{\partial \vec{H}}{\partial t} + \vec{\nabla} \times \left(\frac{\partial v_2}{\partial t} \times \vec{H} \right) \right). \quad (10)$$

Axial component of [equation \(10\)](#)

$$\frac{\partial H_\theta}{\partial t} = \frac{\partial}{\partial r} \left(H_r \frac{\partial v_2}{\partial t} \right) + \frac{\partial}{\partial z} \left(H_z \frac{\partial v_2}{\partial z} \right). \quad (11)$$

It is assumed that the primary magnetic field is uniform throughout the space. It is clear that there is no perturbation in H_r and H_z , but there is perturbation p_2 in H_θ . Then $H_r = H_{01}, H_\theta =$

$H_{02} + p_2$, and $H_z = H_{03}$ where H_{01}, H_{02}, H_{03} are components of the initial magnetic field \vec{H}_0 . As $\vec{H} = (H_0 \cos \phi, p_2, H_0 \sin \phi)$, where $H_0 = |\vec{H}_0|$ and ϕ is the angle at which wave crosses the magnetic field. Thus, \vec{H} can be expressed as:

$$\vec{H} = (H_0 \cos \phi, p_2, H_0 \sin \phi). \quad (12)$$

Here, initially it is assumed that p_2 is zero. Then equations (11) and (12) give:

$$\frac{\partial p_2}{\partial t} = \frac{\partial}{\partial r} \left(H_0 \cos \phi \frac{\partial v_2}{\partial t} \right) + \frac{\partial}{\partial z} \left(H_0 \sin \phi \frac{\partial v_2}{\partial t} \right)$$

Integration of above equation with respect to t gives:

$$p_2 = H_0 \cos \phi \frac{\partial v_2}{\partial r} + H_0 \sin \phi \frac{\partial v_2}{\partial z}. \quad (13)$$

Equation (9) and the relation $\nabla(H^2/2) = -(\vec{\nabla} \times \vec{H}) \times \vec{H} + (\vec{H} \cdot \vec{\nabla})\vec{H}$ give the electromagnetic force as given below:

$$(\vec{J} \times \vec{B}) = \mu_e \left(-\vec{\nabla}(H^2/2) + (\vec{H} \cdot \vec{\nabla})\vec{H} \right).$$

In this case, the components of $(\vec{J} \times \vec{B})$ are $(\vec{J} \times \vec{B})_r = 0$, $(\vec{J} \times \vec{B})_z = 0$, and

$$(\vec{J} \times \vec{B})_\theta = \mu_e H_0^2 \left(\frac{\sin^2 \phi}{r} \frac{\partial^2 v_2}{\partial z^2} + \cos^2 \phi \frac{\partial^2 v_2}{\partial r^2} + \sin \phi \cos \phi \frac{\partial^2 v_2}{\partial r \partial z} + \frac{\sin \phi \cos \phi}{r} \frac{\partial^2 v_2}{\partial r \partial z} \right). \quad (14)$$

For shear harmonic waves, the displacement component $v_2(z)$ can be assumed as:

$$v_2(z) = f_2(z) J_1(kr) e^{i\omega t}. \quad (15)$$

Equations (8), (14) and (15) give:

$$\frac{d^2 f_2}{dz^2} + D_1 \frac{dG_2}{dz} \frac{df_2}{dz} + D_2 f_2 = 0. \quad (16)$$

In equation (16),

$$D_1 = \frac{1}{DG_2} \left(\frac{dG_2}{dz} + \left(1 + \frac{1}{r} \right) \sin \phi \cos \phi J_1'(kr) \right), D = \left(1 + \frac{\mu_2 \mu_e H_0^2 \sin^2 \phi}{G_2} \right),$$

$$D_2 = \frac{1}{DG_2} \left(k^2 \left(\frac{\mu_2}{G_2} + \mu_2 \mu_e H_0^2 \cos^2 \phi \right) J_1''(kr) + \omega^2 \left(\frac{\rho_{1100} \rho_{2200} - \rho_{1200}^2}{\rho_{2200}} \right) \right), G_2 = \mu_2 - \frac{P_2}{2},$$

$$\mu_2 = \mu_{20}(1 + qz)^2, P_2 = P_{20}(1 + qz)^2, \rho_{1100} = \rho_{11001}(1 + qz)^2,$$

$$\rho_{1200} = \rho_{12001}(1 + qz)^2, \rho_{2200} = \rho_{22001}(1 + qz)^2, \xi_{20} = P_{20}/2\mu_{20}. \quad (17)$$

The solution of equations (16) and (15) give:

$$v_2(z) = \exp(-D_1 z/2) (C_3 \cos(\chi_2 z) + C_4 \sin(\chi_2 z)) J_1(kr) e^{i\omega t},$$

Here, $\chi_2 = D_2^2$, C_3, C_4 are arbitrary constants. Substitution of above displacement component in [equation \(2\)](#) gives the following stress component in the medium under consideration:

$$(\sigma_{\theta z})_{M_2} = C_3 \left(\left(\mu_{20}(1 + qz)^2 \exp(-D_1 z/2) \right) \left(\cos(\chi_2 z) \chi_2 - (D_1/2) \sin(\chi_2 z) J_1(kr) \right) \right) \\ + C_4 \left(\left(\mu_{20}(1 + qz)^2 \exp(-D_1 z/2) \right) \left(\sin(\chi_2 z) \chi_2 - (D_1/2) \cos(\chi_2 z) J_1(kr) \right) \right)$$

3.3 The lower poroelastic medium ($z > 0$)

In the lower heterogeneous poroelastic half space, let (u_3, v_3, w_3) and (U_3, V_3, W_3) be the solid and fluid displacement components, respectively. For shear wave in this space, the equation of motion (1) takes the following form

$$\mu_3(z) \left(\frac{\partial^2 v_3}{\partial r^2} + \frac{1}{r} \frac{\partial v_3}{\partial r} - \frac{v_3}{r^2} \right) + \frac{\partial}{\partial z} \left(G_3 \frac{\partial v_3}{\partial z} \right) = \frac{\partial^2}{\partial t^2} (\rho_{11000} v_3 + \rho_{12000} V_3), \\ 0 = \frac{\partial^2}{\partial t^2} (\rho_{12000} v_3 + \rho_{22000} V_3). \quad (18)$$

In [equation \(18\)](#), $\mu_3 = \mu_{30}(1 + l_1 z)$, $G_3 = \mu_3(1 - P_3/2)$, $P_3 = P_{30}(1 + l_3 z)$, $\xi_{30} = P_{30}/2\mu_{30}$, $\rho_{11000} = \rho_{110001}(1 + l_2 z)$, $\rho_{12000} = \rho_{120001}(1 + l_2 z)$, $\rho_{22000} = \rho_{220001}(1 + l_2 z)$. μ_{30} , P_{30} , ρ_{110001} , ρ_{120001} , ρ_{220001} , are the initial values of the respective parameters. The non-zero stress components are $\sigma_{r\theta} = \mu_3(z) \left(\frac{\partial v_3}{\partial r} - \frac{v_3}{r} \right)$, $\sigma_{z\theta} = \mu_3(z) \left(\frac{\partial v_3}{\partial z} \right)$. As in earlier cases, the solution of [equation \(18\)](#) $v_3(z)$ assumed as:

$$v_3(z) = f_3(z) J_1(kr) e^{i\omega t}. \quad (19)$$

[Equations \(18\)](#) and [\(19\)](#) give:

$$\frac{d^2 f_3}{dz^2} + \frac{1}{G_3} \frac{dG_3}{dz} \frac{df_3}{dz} - \frac{k^2 \mu_3}{G_3} \left(1 - \frac{c^2}{\beta_3^2} \right) f_3 = 0, \quad (20)$$

In [equation \(20\)](#), $\beta_3 = \left(\frac{\mu_{30} \rho_{22000}}{\rho_{11000} \rho_{22000} - \rho_{12000}^2} \right)^{1/2}$,

To make nonlinear [equation \(20\)](#) linear, assume that

$$f_3(z) = \frac{f_{30}(z)}{\sqrt{G_{30}(1 + l_4 z)}}, \quad (21)$$

here $f_{30}(z)$ is an arbitrary function, $G_{30} = \mu_{30}(1 - \xi_{30})$, $l_4 = l_1 - \xi_{30} l_3/1 - \xi_{30}$. Then [equation \(20\)](#) reduces to:

$$\frac{d^2 f_{30}}{dz^2} + \left[\frac{l_4^2}{4(1 + l_4 z)^2} - k_3^2 \left(\frac{(1 + l_1 z)}{(1 + l_4 z)} - \frac{c^2(1 + l_2 z)}{\beta_3^2(1 + l_4 z)} \right) \right] = 0. \quad (22)$$

Introducing $\eta = \frac{2\chi_3 k_3}{l_4}(1 + l_4 z)$, here $\chi_3 = \left[\frac{1}{l_4} \left(l_1 - \frac{c^2}{\beta_3^2} l_2 \right) \right]^{\frac{1}{2}}$, $k_3^2 = k^2 \mu_{30}/G_{30}$, and substituting $f_{30}(z) = \phi(\eta)$, [equation \(22\)](#) becomes:

$$\phi''(\eta) + \left(\frac{1}{4\eta^2} + \frac{R}{\eta} - \frac{1}{4} \right) \phi(\eta) = 0. \quad (23)$$

In [equation \(23\)](#), $R = \frac{k_3}{2\chi_3 l_4} \left[\left(\frac{c^2}{\beta_3^2} - 1 \right) + \chi_3^2 \right]$, $\chi_3 = \left[\frac{1}{l_4} \left(l_1 - \frac{l_2 c^2}{\beta_3^2} \right) \right]^{\frac{1}{2}}$, [equation \(23\)](#) is the well-known form of Whittaker equation (34). The solution of [equation \(23\)](#) $\phi(\eta) = C_5 W_{R,0}(\eta) + C_6 W_{-R,0}(-\eta)$. $W_{R,0}$, $W_{-R,0}$ are Whittaker functions, C_5, C_6 are arbitrary constants. For bounded solution, C_6 must be zero. In this case, the solution of [equation \(20\)](#) is:

$$f_3(z) = C_5 \left[W_{R,0} \left(\frac{2\chi_3 k_3}{l_4} (1 + l_4 z) \right) \right] \frac{1}{\sqrt{G_{30}(1 + l_4 z)}} J_1(kr) e^{i\omega t}. \quad (24)$$

Using [equations \(24\)](#) and [\(19\)](#) in [equation \(2\)](#), the pertinent stress is given by:

$$\begin{aligned} (\sigma_{\theta z})_{M_3} = C_5 & \left[\left(\mu_3 l_4 / G_{30} (1 + l_4 z)^{1/2} \right) \left[\left(l_4 (R - z/2) / G_{30} (1 + l_4 z)^{1/2} \right) \right. \right. \\ & \left. \left. W_{R,0} (2\chi_3 k_3 (1 + l_4 z) / l_4) + (R - 1/2)^2 W_{R-1,0} (2\chi_3 k_3 (1 + l_4 z) / l_4) \right] \right. \\ & \left. - \left(l_4 / 2 G_{30} (1 + l_4 z)^{3/2} \right) W_{R,0} (2\chi_3 k_3 (1 + l_4 z) / l_4) \right]. \end{aligned}$$

4. Boundary conditions and frequency equation

The boundary conditions at free boundary and two interfaces are prescribed as follows:

Assume that $z = -h_2$ is stress free if $(\sigma_{\theta z})_{M_1} = 0$, at $z = -h_1$, the displacement and stress must be continuous, i.e. $(\sigma_{\theta z})_{M_1} = (\sigma_{\theta z})_{M_2}$, $v_1 = v_2$, and at the plane of contact of the magneto poroelastic medium and poroelastic half space, i.e. at $z = 0$ the displacement and stress must be continuous, i.e. $(\sigma_{\theta z})_{M_2} = (\sigma_{\theta z})_{M_3}$, $v_2 = v_3$. These boundary conditions lead to the following system of homogeneous equations:

$$[A_{ij}] [C_i] = [0]_{2,2} i = 1, 2, 3, 4, 5. \quad (25)$$

[Equation \(25\)](#) results in a system of five homogeneous equations in five arbitrary constants C_1, C_2, C_3, C_4, C_5 . To obtain a non-trivial solution, the determinant of coefficients must be zero. Accordingly, the following frequency equation is obtained.

$$|A_{ij}| = 0, i, j = 1, 2, 3, 4, 5. \quad (26)$$

5. Particular cases

Case (i): In the sandwiched medium if the magnetic and porous properties are absent, then the problem is reduced to that of classical elasticity ([Paswan et al., 2017](#)), and the frequency [equation \(26\)](#) is:

EC

$$\begin{vmatrix} 0 & A_{10} & B_{10} \\ A_{20} & B_{20} & 0 \\ A_{30} & B_{30} & C_{30} \end{vmatrix} = 0. \quad (27)$$

In [equation \(27\)](#),

$$A_{10} = \chi_{10} J_1(kr), B_{10} = \frac{l_4(R)}{G_{30}} W_{R,0} \left(\frac{2k_3}{l_4} \right), A_{20} = S_3 \chi_{10} J_1(kr), B_{20} = \mu_T S_2 k'_1(kr) - S_3 \frac{E}{2} J_1(kr),$$

$$A_{30} = e^{\frac{-\beta h}{2}} \sin(\chi_{10} h_1) J_1(kr), B_{30} = e^{\frac{-\beta h_1}{2}} \cos(\chi_{10} h_1) J_1(kr), C_{30} = \left[W_{R,0} \left(\frac{2\chi_{30} k_3}{l_4} (1 + l_4 h_1) \right) \right] \frac{1}{\sqrt{G_{30}(1 + l_4 h_1)}} J_1(kr),$$

$$\chi_{10} = - \left(\frac{J_1''(kr) k^2}{\xi_{10} J_1(kr)} + \frac{J_1'(kr) k}{\xi_{10} r J_1(kr)} + \omega^2 \left(\frac{\rho_{110}}{\mu J_1(kr)} \right) \right).$$

$$\chi_{30} = \left[\frac{1}{l_4} \left(l_1 - \frac{c^2}{\beta_3^2} l_2 \right) \right]^{\frac{1}{2}},$$

$$\beta_3 = \left(\frac{\mu_{30}}{\rho_{11000}} \right)^{1/2},$$

Case (ii): When the inhomogeneity parameter is absent, i.e. for upper layer $a \rightarrow 0, \mu_L = \mu_T = \mu$, for intermediate layer $q \rightarrow 0$, and for lower poroelastic half space $l_1 \rightarrow 0, l_2 \rightarrow 0, l_3 \rightarrow 0$, then the frequency [equation \(26\)](#) reduces to:

$$\begin{vmatrix} 0 & A_{11} \sin(\chi_{11} h_2) & 0 \\ 0 & A_{11} \sin(\chi_{11} h_1) & A_{21} \\ A_{31} \cos(\chi_2 h_1) & A_{31} \sin(\chi_2 h_1) & A_{41} \end{vmatrix}. \quad (28)$$

In [equation \(28\)](#),

$$A_{11} = \chi_{11} J_1(kr),$$

$$\chi_{11} = - \left(\frac{J_1''(kr) k^2}{\xi_{10} J_1(kr)} + \frac{J_1'(kr) k}{\xi_{10} r J_1(kr)} - \frac{1}{\xi_{10} r^2} + \omega^2 \left(\frac{\rho_{1100} \rho_{2200} - \rho_{1200}^2}{\xi_{10} \rho_{2200} \mu J_1(kr)} \right) \right),$$

$$A_{21} = \mu_{20} e^{-D_1 h_1/2} (\chi_2 - D_1 h_1/2) J_1(kr), A_{31} = J_1(kr), A_{41} = e^{-D_1 h_1/2} J_1(kr).$$

μ_{20}, D_1 , are similar expressions as [equation \(17\)](#) with $q \rightarrow 0$.

Case (iii): Apart from the conditions of case (ii), if the initial stress is absent, i.e. for upper layer $P_1 \rightarrow 0, \xi_{10} \rightarrow 0$, for intermediate layer $P_2 \rightarrow 0, \xi_{20} \rightarrow 0, G_{20} \rightarrow \mu_{20}$, and for lower poroelastic half space $P_3 \rightarrow 0, \xi_{30} \rightarrow 0, G_{30} \rightarrow \mu_{30}, k_3 \rightarrow k$.

Then the frequency [equation \(26\)](#) reduces to:

$$\begin{vmatrix} 0 & B_{12} \sin(\chi_{12} h_2) & 0 \\ 0 & B_{12} \sin(\chi_{12} h_1) & A_{22} \\ A_{32} \cos(\chi_2 h_1) & A_{32} \sin(\chi_2 h_1) & A_{42} \end{vmatrix} = 0. \quad (29)$$

In [equation \(29\)](#),

$$B_{12} = \chi_{12} J_1(kr),$$

$$\chi_{12} = \frac{J_1''(kr)k^2}{J_1(kr)} + \frac{J_1'(kr)k}{rJ_1(kr)} - \frac{1}{r^2} + \omega^2 \left(\frac{\rho_{1100}\rho_{2200} - \rho_{1200}^2}{\rho_{2200}\mu J_1(kr)} \right),$$

The other expressions for [equation \(29\)](#) are similar to that of [equation \(28\)](#) with $P_2 \rightarrow 0$.

6. Numerical results

For numerical process, the following materials are used.

The material parameters for upper self-reinforced medium ([Chattaraj and Samal, 2013](#)) (Say Mat-I), are:

$$\mu^T = 2.46 \times 10^9 \text{ N/m}^2, \mu_L = 5.66 \times 10^9 \text{ N/m}^2, \rho_{110} = 1.92637 \times 10^3 \text{ kg/m}^3$$

$$\rho_{120} = -0.002137 \times 10^3 \text{ kg/m}^3, \rho_{220} = 0.215337 \times 10^3 \text{ kg/m}^3$$

The intermediate magneto poroelastic medium is assumed to be sandstone saturated with kerosene ([Yew and Jogi, 1976](#)) (Say Mat-II). The values in this case are $\mu_{20} = 70199 \times 10^{10} \text{ N/m}^2$, $\rho_{1100} = 24152 \times 10^3 \text{ kg/m}^3$, $\rho_{1200} = -300 \text{ kg/m}^3$, $\rho_{2200} = 500 \times 10^3 \text{ kg/m}^3$.

The lower half-space is assumed to be sandstone saturated with water ([Fatt, 1959](#)) (Say Mat-III). The values in this case are $\mu_{30} = 0.92 \times 10^{10} \text{ N/m}^2$, $\rho_{11000} = 1.9002 \times 10^3 \text{ kg/m}^3$, $\rho_{12000} = 0$, $\rho_{22000} = 0.2268 \times 10^3 \text{ kg/m}^3$.

Using these values in the frequency equation, the implicit relation between the phase velocity and wavenumber is obtained. Phase velocity is computed against wavenumber. The magneto-poroelastic coupling factor is taken to be $\mu_e H_0^2 / N = 0.01$ ([Balu et al., 2017](#)). Moreover, the values for ϕ, kr are taken to be $\pi/6, 5$ ([Chattopadhyay et al., 2012](#)) and the other parameter values are in various cases specified in [Table 1](#). The values are computed using the bisection method implemented in MATLAB, and the results are depicted in [Figures 2-6](#).

	ah_1	$l_1 h_1$	$l_2 h_1$	$l_3 h_1$	qh_1	ξ_{10}	ξ_{20}	ξ_{30}	h_2/h_1	μ_l/μ_t
Figure 2	0.4	0.5	0.4	0.3	0.4	0.4	0.3	0.2	—	1.2
Figure 3	—	0.5	0.4	0.3	0.4	0.4	0.3	0.2	1.6	1.2
Figure 4	—	0.5	0.4	0.3	0.4	0.4	0.3	0.2	1.6	—
Figure 5	0.4	0.5	0.4	0.3	—	—	0.3	0.2	1.6	1.2
Figure 6	0.4	0.5	0.4	0.3	0.4	—	0.3	0.2	1.6	1.2

Table 1.
Parameter values

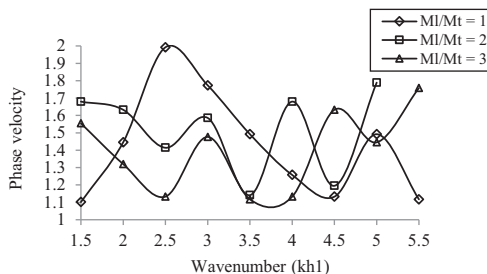


Figure 2.
Variation of phase
velocity with
wavenumber for
various values (μ_l/μ_t) in upper
reinforcement
medium

Figure 3.
Variation of phase velocity with wavenumber for various ratios (h_2/h_1)

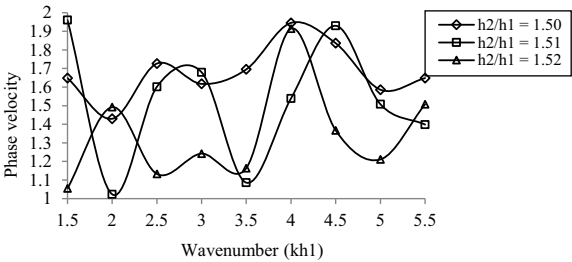


Figure 4.
Variation of phase velocity with wavenumber for various values of inhomogeneity parameter (ah_1) in upper reinforcement medium

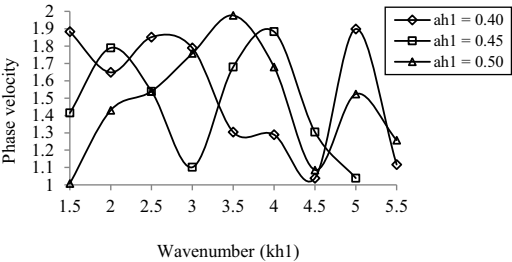


Figure 5.
Variation of phase velocity with wavenumber for various values of inhomogeneity parameter (qh_1) in magneto poroelastic medium

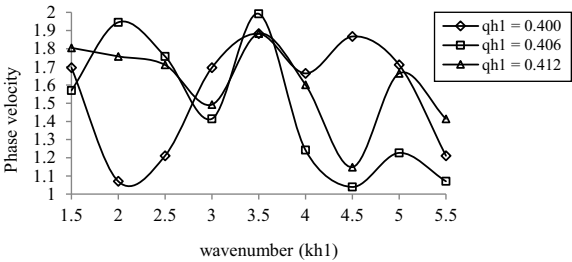


Figure 6.
Variation of phase velocity with wavenumber for various values of heterogeneity parameter (χ_{10}) in elastic medium

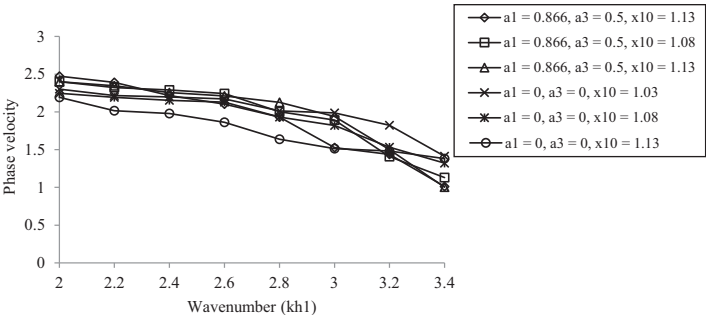


Figure 2 depicts the variation of phase velocity with wavenumber for different values of (μ_L/μ_T) in upper reinforcement medium. From this figure, it is clear that, as wavenumber increases, phase velocity, in general, decreases. The notations $M1/Mt = 1, M1/Mt = 2, M1/Mt = 3$ used in the Figure 2 represent the different values of (μ^L, μ^T) . Figure 3 depicts the variation of phase velocity with wavenumber for different values of (h_2/h_1) . From Figure 3, it is seen that as wavenumber increases, phase velocity, in general, decreases. Figure 4 depicts the variation of phase velocity with wavenumber for various inhomogeneity parameter values in upper reinforcement medium. From this figure, it is observed that, as wavenumber increases, phase velocity, in general, decreases for all values of inhomogeneity parameter (ah_1) . Figure 5 depicts the variation of phase velocity with wavenumber for various inhomogeneity parameter values in magneto poroelastic medium. From this figure, it is clear that, as wavenumber increases, phase velocity, in general, increases when the inhomogeneity parameter $qh_1 = 0.400$, whereas when $qh_1 = 0.406, 0.412$, phase velocity, in general, decreases. For the validation, the results are computed for particular case (i). Phase velocity is computed against the wavenumber for various heterogeneity parameters in presence of reinforcement and free from reinforcement. The results are presented in Figure 6. In Figure 6, Curves 1, 2 and 3 pertaining to presence of reinforcement, whereas the Curves 4, 5 and 6 pertaining to free from reinforcement for the steel (Paswan *et al.*, 2017). From this figure, it is clear that as wavenumber increases phase velocity decreases as the values of heterogeneity parameter (χ_{10}) increases in both reinforced and reinforced free cases. These results are in agreement with that of the paper (Paswan *et al.*, 2017).

7. Conclusion

Shear wave propagation in magneto poroelastic medium embedded between a self-reinforced medium and poroelastic half space are investigated in presence of initial stress, and inhomogeneity parameter. For heterogeneous poroelastic half space, the Whittaker's solution is obtained. From the numerical results, it is observed that heterogeneity parameter, inhomogeneity parameter and reinforcement parameter have significant influences on the wave characteristics. In addition, frequency equation is discussed in absence of inhomogeneity and initial stress. For the validation purpose, numerical results are also computed for a particular case.

References

- Abd-Alla, A., Nofal, T., Abo-Dahab, S. and Al-Mullise, A. (2013), "Surface wave propagation in fiber-reinforced anisotropic elastic media subjected to gravity field", *International Journal of Physical Sciences*, Vol. 8 No. 14, pp. 574-584.
- Alimirzaei, S., Mohammedmechr, M. and Tounsi, A. (2019), "Nonlinear analysis of viscoelastic micro-composite beam with geometrical imperfection using FEM: MSGT electro-magneto-elastic bending, buckling and vibration solutions", *Structural Engineering and Mechanics*, Vol. 59 No. 3, pp. 485-502.
- Balu, C., Rajitha, G., Ramesh, M. and Reddy, P.M. (2017), "Shear wave propagation in magneto-poroelastic dissipative isotropic medium sandwiched between two poroelastic half spaces", *International Journal of Pure and Applied Mathematics*, Vol. 118 No. 20, pp. 4645-4656.
- Belfield, A.J., Rogers, T.G. and Spencer, A.J.M. (1983), "Stress in elastic plates reinforced by fibers lying in concentric circles", *Journal of the Mechanics and Physics of Solids*, Vol. 31 No. 1, pp. 25-54.
- Biot, M.A. (1956), "Theory of propagation of elastic waves in a fluid – saturated porous solid-I", *The Journal of the Acoustical Society of America*, Vol. 28 No. 2, pp. 168-178.

- Boukhelif, Z., Bouremana, M., Bourada, F., Bousahla, A.A., Bourada, M., Tounsi, A. and Al-Osta, M.A. (2019), "A simple quasi-3D HSDT for the dynamics analysis of FG thick plate on elastic foundation", *Steel and Composite Structures*, Vol. 31 No. 5, pp. 503-516.
- Cahudhary, S., Kaushik, V.P. and Tomar, S.K. (2006), "Plane SH wave response from elastic slab interposed between two different self-reinforced elastic solids", *International Journal of Applied Mechanics and Engineering*, Vol. 11 No. 4, pp. 787-801.
- Chattaraj, R. and Samal, S.K. (2013), "Love waves in the fiber-reinforced layer over a gravitating porous half space", *Acta Geophysica*, Vol. 61 No. 5, pp. 1170-1183.
- Chatterjee, M., Sudarshan, D. and Chattopadhyay, A. (2015), "Propagation of shear waves in viscoelastic heterogeneous layer overlying an initially stressed half-space", *International Conference on Vibration Problems (ICOVP-2015)*, *Journal of Physics: Conference Series* 662, IOP Publishing, doi: [10.1088/1742-6596/662/1/012001](https://doi.org/10.1088/1742-6596/662/1/012001).
- Chattopadhyay, A. and Chaudhury, S. (1995), "Magneto elastic shear waves in an infinite self-reinforced plate", *International Journal for Numerical and Analytical Methods in Geomechanics*, Vol. 19 No. 4, pp. 289-304.
- Chattopadhyay, A. and Singh, A.K. (2012), "Propagation of magneto elastic shear waves in an irregular self-reinforcement layer", *Journal of Engineering Mathematics*, Vol. 75 No. 1, pp. 139-155.
- Chattopadhyay, A., Gupta, S. and Singh, A.K. (2010), "The dispersion of shear wave in multilayered magneto elastic self-reinforced media", *International Journal of Solids and Structures*, Vol. 47 No. 9, pp. 1317-1324.
- Chattopadhyay, A., Gupta, S., Sahu, S. and Singh, A. (2012), "Torsional surface waves in a self-reinforced medium over a heterogeneous half space", *International Journal of Geomechanics*, Vol. 12 No. 2, pp. 193-197.
- Chattopadhyay, A., Gupta, S., Singh, A.K. and Sanjeev Sahu, A. (2011), "Effect of point source self-reinforcement and heterogeneity on the propagation of magneto elastic shear waves", *Applied Mathematics*, Vol. 2 No. 3, pp. 271-282.
- Fahmy, M.A. (2012a), "The effect of rotation and inhomogeneity on the transient magneto-thermo viscoelastic stresses in an anisotropic solid", *Journal of Applied Mechanics*, Vol. 79 No. 5, pp. 10-15.
- Fahmy, M.A. (2012b), "Time stepping DRBEM for the transient magneto-thermo-visco-elastic stresses in a rotating non-homogeneous anisotropic solid", *Engineering Analysis with Boundary Elements*, Vol. 36 No. 3, pp. 335-345.
- Fahmy, M.A. (2012c), "Transient magneto thermo viscoelastic plane waves in a non-homogeneous anisotropic thick strip subjected to a moving heat source", *Applied Mathematical Modelling*, Vol. 36 No. 10, pp. 4565-4578.
- Fahmy, M.A. (2012d), "Transient magneto-thermo elastic stresses in an anisotropic viscoelastic solid with and without moving heat source", *Numerical Heat Transfer, Part A: Applications*, Vol. 61 No. 8, pp. 547-564.
- Fahmy, M.A. (2013), "A three dimensional generalized magneto-thermo-viscoelastic problem of a rotating functionally graded anisotropic solids with and without energy dissipation", *Numerical Heat Transfer, Part A: Applications*, Vol. 63 No. 9, pp. 713-733.
- Fatt, I. (1959), "The Biot-Willis elastic coefficients for sandstone", *Journal of Applied Mechanics*, Vol. 26, pp. 296-297.
- Karami, B., Shahsavari, D., Janghorban, M. and Tounsi, A. (2019a), "Resonance behavior of functionally graded polymer composite nanoplates reinforced with graphene nanoplates", *International Journal of Mechanical Sciences*, Vol. 156, pp. 94-105.
- Karami, B., Shahsavari, D., Janghorban, M. and Tounsi, A. (2019b), "On prestressed functionally graded anisotropic nanoshell in magnetic field", *Journal of the Brazilian Society of Mechanical Sciences and Engineering*, Vol. 41 No. 11, p. 495.
- Kr Mukhopadhyay, A., Kr Gupta, A. and Kundu, S. (2017), "Influence of initial stress and gravity on torsional surface wave in heterogeneous medium", *Journal of Vibration and Control*, Vol. 23 No. 6, pp. 970-979.

- Medani, M., Benahmed, A., Zidour, M., Heireche, H., Tounsi, A., Bousahla, A.A., Tounsi, A. and Mahmoud, S.R. (2019), "Static and dynamic behavior of (FG-CNT) reinforced porous sandwich plate", *Steel and Composite Structures*, Vol. 32 No. 5, pp. 595-610.
- Paswan, B., Sahu, S.A. and Saroj, P.K. (2017), "Dynamic response of heterogeneity and reinforcement on the propagation of torsional surface waves", *Technische Mechanik*, Vol. 37 No. 1, pp. 69-81.
- Roy, I., Acharya, D.P. and Acharya, S. (2017), "Propagation and reflection of plane waves in a rotating magneto elastic fibre-reinforced semi space with surface stress", *Mechanics and Mechanical Engineering*, Vol. 21 No. 4, pp. 1043-1061.
- Samal, S.K. and Chattaraj, R. (2011), "Surface wave propagation in fiber-reinforced anisotropic elastic layer between liquid saturated porous half space and uniform liquid layer", *Acta Geophysica*, Vol. 59 No. 3, pp. 470-482.
- Singh, A.K., Das, A., Anirban, L. and Chattopadhyay, A. (2016), "Effect of corrugation and reinforcement on the dispersion of SH-wave propagation in corrugated poroelastic layer lying over a fibre reinforced half-space", *Acta Geophysica*, Vol. 64 No. 5, pp. 1340-1369.
- Tlidji, Y., Zidour, M., Draiche, K., Safa, A., Bourada, M., Tounsi, A., Bousahla, A.A. and Mahmoud, S.R. (2019), "Vibration analysis of different material distributions of functionally graded microbeam", *Structural Engineering and Mechanics*, Vol. 69 No. 6, pp. 637-649.
- Tong, L.H., Yu, Y., Hu, W.T., Shi, Y.F. and Xu, C.J. (2016), "On wave propagation characteristics in fluid saturated porous materials by a nonlocal Biot theory", *Journal of Sound and Vibration*, Vol. 379, pp. 106-118.
- Tong, L.H., Lai, S.K., Zeng, L.L., Xu, C.J. and Yang, J. (2018), "Nonlocal scale effect on Rayleigh wave propagation in porous fluid-saturated materials", *International Journal of Mechanical Sciences*, Vol. 148, pp. 459-466.
- Vardoulakis, I. (1984), "Torsional surface waves in inhomogeneous elastic media", *International Journal for Numerical and Analytical Methods in Geomechanics*, Vol. 8 No. 3, pp. 287-296.
- Verma, P. (1986), "Magneto elastic shear waves in self-reinforced bodies", *International Journal of Engineering Science*, Vol. 24 No. 7, pp. 1067-1073.
- Verma, P., Rana, O. and Verma, M. (1988), "Magneto elastic transverse surface waves in self-reinforced elastic bodies", *Indian Journal of Pure and Applied Mathematics*, Vol. 19 No. 7, pp. 713-716.
- Yew, C.H. and Jogi, P.N. (1976), "Study of wave motions in fluid-saturated porous rocks", *Journal of Acoustical Society of America*, Vol. 60 No. 1, pp. 2-8.

Further reading

Whittaker, E.T. and Watson, G.N. (1991), *A Course of Modern Analysis*, Cambridge University Press, Cambridge, New York, NY.

Corresponding author

Rajitha Gurijala can be contacted at: rajitha.akshu@gmail.com

For instructions on how to order reprints of this article, please visit our website:

www.emeraldgrouppublishing.com/licensing/reprints.htm

Or contact us for further details: permissions@emeraldinsight.com